Reversible Redox- and Zinc-Dependent Dimerization of the *Escherichia coli* Fur Protein

Benoît D'Autréaux,[‡] Ludovic Pecqueur,[‡,§] Anne Gonzalez de Peredo,[||] Rutger E. M. Diederix,[‡] Christelle Caux-Thang,[‡] Lyes Tabet,[‡] Beate Bersch,[§] Eric Forest,[||] and Isabelle Michaud-Soret*[,‡]

Laboratoire de Physicochimie des Métaux en Biologie, UMR 5155 CNRS/CEA/UJF, Département Réponse et Dynamique Cellulaires, CEA-Grenoble, 17 avenue des Martyrs, 38054 Grenoble cedex 9, France, and Laboratoire de Spectrométrie de Masse des Protéines and Laboratoire de RMN des Protéines, Institut de Biologie Structurale, Jean-Pierre Ebel, UMR 5075 CNRS/CEA/UJF, F-38027 Grenoble Cedex 1, France

Received August 11, 2006; Revised Manuscript Received December 4, 2006

ABSTRACT: Fur is a bacterial regulator using iron as a cofactor to bind to specific DNA sequences. This protein exists in solution as several oligomeric states, of which the dimer is generally assumed to be the biologically relevant one. We describe the equilibria that exist between dimeric *Escherichia coli* Fur and higher oligomers. The dissociation constant for the dimer−tetramer equilibrium is estimated to be in the millimolar range. Oligomerization is enhanced at low ionic strength and pH. The as-isolated monomeric form of Fur is not in equilibrium with the dimer and contains two disulfide bridges (C92−C95 and C132−C137). Binding of the monomer to DNA is metal-dependent and sequence specific with an apparent affinity 5.5 times lower than that of the dimer. Size exclusion chromatography, EDC cross-linking, and CD spectroscopy show that reconstitution of the dimer from the monomer requires reduction of the disulfide bridges and coordination of Zn^{2+}. Reduction of the disulfide bridges or Zn^{2+} alone does not promote dimerization. EDC and DMA cross-links reveal that the N-terminal NH_2 group of one subunit is in an ionic interaction with acidic residues of the C-terminal tail and close to Lys76 and Lys97 of the other. Furthermore, the yields of cross-link drastically decrease upon binding of metal in the activation site, suggesting that the N-terminus is involved in the conformational change. Conversely, oxidizing reagents, H_2O_2 or diamide, disrupt the dimeric structure leading to monomer formation. These results establish that coordination of the zinc ion and the redox state of the cysteines are essential for holding *E. coli* Fur in a dimeric state.

Fur[1] (ferric uptake regulation protein) is a global regulator ubiquitous in Gram-negative bacteria which controls the expression of more than 90 genes in *Escherichia coli* (*1*). This dimeric protein (2 × 17 kDa) was initially described as a key protein for the control of intracellular iron concentration (*2*−*4*). When cellular iron concentrations become sufficiently high, the Fur repressor binds ferrous iron, its corepressor, which activates its DNA binding activity to specific DNA sequences called "iron box", leading to transcriptional repression of genes involved in iron uptake (*5*, *6*). The role of Fur is linked not only to the availability of iron but also to the response to various stresses in which iron is intimately involved. For instance, Fur is involved in response to oxidative (*4*), nitrosative (*7*−*9*), and acid stress (*10*, *11*).

The Fur protein appears mainly as a dimer (Fur_D) in solution according to HPLC experiments (*12*) and mass spectrometry data (*13*). Complementation experiments with inactive mutants suggest that the active form of Fur is at least a dimer in vivo (*14*). Furthermore, the free protein and the protein bound to DNA are able to oligomerize in a pH-dependent way as observed by electron microscopy (*15*, *16*). The polymerization on DNA may be linked to the tuning of the regulation response by Fur (*17*).

The first X-ray structure of a Fur protein has been reported recently, with the Fur protein of *Pseudomonas aeruginosa* (*18*). The protein was crystallized, in the presence of an excess of zinc, as a homodimer. The structure shows that the protein contains a winged helix−turn−helix DNA binding motif and a dimerization domain. As expected from previous extensive studies of *E. coli* Fur (*19*−*22*), two relevant metal binding sites were identified in the crystal

* To whom correspondence should be addressed: Laboratoire de Physicochimie des Métaux en Biologie, Département de Réponses dynamique et cellulaire, CEA-Grenoble, 17 avenue des Martyrs, 38054 Grenoble cedex 9, France. Telephone: (33) 4 38 78 99 40. Fax: (33) 4 38 78 34 62. E-mail: imichaud@cea.fr.

‡ CEA-Grenoble.

§ Laboratoire de RMN des Protéines, Institut de Biologie Structurale, Jean-Pierre Ebel, UMR 5075 CNRS/CEA/UJF.

|| Laboratoire de Spectrométrie de Masse des Protéines, Institut de Biologie Structurale, Jean-Pierre Ebel, UMR 5075 CNRS/CEA/UJF.

[1] Abbreviations: Fur, ferric uptake regulation protein; EDTA, ethylenediaminotetraacetic acid; PMSF, phenylmethanesulfonyl fluoride; Mes, 2-(*N*-morpholino)ethanesulfonic acid; MOPS, morpholinopropanesulfonic acid; BTP and Bis-Tris propane, 1,3-bis[tris(hydroxymethyl)methylamino]propane; Tris, tris(hydroxymethyl)aminomethane; ESI-MS, electrospray ionization mass spectrometry; Fur-Met, Fur protein without the N-terminal methionine; MALDI-TOF, matrix-assisted laser desorption ionization time of flight; HPLC, high-pressure liquid chromatography; LC, liquid chromatography; EDC, 1-ethyl 3-[3-(dimethylamino)propyl]carbodiimide. Terminology used to describe the metal-containing form and oligomeric state of Fur: M_1Fur_D, dimeric Fur with metal in the structural high-affinity site; $M_1M_2Fur_D$, dimeric Fur metal metal in the structural high-affinity site and in the regulatory site; Fur_M^{SS}, oxidized monomeric Fur; Fur_M^{SH}, reduced monomeric Fur.

10.1021/bi061636r CCC: $37.00
Published on Web 01/12/2007

structure: a regulatory site responsible for activation of the DNA binding activity and a purported high-affinity zinc site. In the regulatory site, the zinc ion is hexacoordinated in an octahedral geometry, with a water molecule occupying one of these positions. Spectroscopic data (EPR, Mössbauer, and X-ray absorption) obtained with the iron-containing form of *E. coli* Fur, the physiologically relevant form, are in agreement with the crystallographic structure, indicating that the structure of this site may be very similar when iron is bound (*22*). The high-affinity zinc site in *P. aeruginosa* Fur contains a zinc ion in a tetrahedral geometry coordinated by two histidines (H32 and H89) and two glutamates (E80 and E100). In contrast, for *E. coli* Fur (Zn_1Fur_D), EXAFS studies showed that the zinc ion is coordinated by two cysteines and one or two aspartates or one histidine and one aspartate (*19*). The two cysteines, C92 and C95, have been identified as ligands of the zinc atom using chemical modification and mass spectrometry (*23*). This confirmed the importance of these two cysteines which have been shown to be essential to the *E. coli* Fur activity by site-directed mutagenesis (*24*). These cysteines are conserved in a large number of Fur proteins, but only one is conserved in *P. aeruginosa* Fur. This one was shown to be dispensable for the in vivo activity of *P. aeruginosa* Fur by site-directed mutagenesis (*25*). These data provide evidence that the zinc site probably plays a structural role but is not strictly conserved among the Fur proteins, although to date no clear explanation of the role of this zinc site variability has been found.

In this work, we have focused on the characterization of the different oligomeric forms of the *E. coli* Fur protein. The oligomeric properties of Fur are described, as a function of ionic strength and pH. Furthermore, we observe that formation of two intramolecular disulfide bridges can lock Fur in a monomeric state (Fur_M^{SS}) and that dimerization is induced by binding of zinc after reduction of the cysteines. Therefore, we propose that the high-affinity zinc ion is a structural zinc ion essential for dimerization of *E. coli* Fur and is involved in the control of the cysteine redox state. Cross-linking experiments have allowed us to identify amino acids of the Fur protein involved in intersubunit contacts and in their proximity. Altogether, these data allow us to progress in the understanding of the structural properties of the Fur protein in solution that are potentially linked to the response to various types of stress, especially acid stress and oxidative stress, which will be discussed.

EXPERIMENTAL PROCEDURES

Chemicals. Trizma, Bis-Tris propane, MOPS and Mes buffers, ethylenediaminetetraacetic acid (EDTA), triethanolamine, 1-ethyl 3-[3-(dimethylamino)propyl]carbodiimide (EDC), dimethyl adipimidate (DMA), diamide, $ZnSO_4$, $MnSO_4$, and $MgSO_4$ were purchased from Sigma/Aldrich. Chymotrypsin, endoproteinase Lys-C, and endoproteinase Glu-C were purchased from Boehringer Mannheim. Immobilized pepsin was purchased from Pierce.

Overproduction and Purification of Fur. Fur was overproduced and purified as previously described (*26*) but with some modifications (*7*). A higher yield (up to 40%) in monomeric Fur can be obtained by increasing the EDTA concentration in the extraction buffer to 100 mM. The samples collected via gel filtration (Superdex 75 from Amersham Biosciences) were concentrated in 100 mM Tris-HCl containing 100 mM KCl and 10% (v/v) glycerol at pH 8. Protein concentrations, consistently expressed in subunit concentration unless indicated otherwise, were determined spectrophotometrically using an absorption coefficient of 0.4 $mg^{-1}\ mL^{-1}\ cm^{-1}$ at 275 nm for one monomer of pure native Fur (*26*).

Analysis of Oligomeric Forms by Size Exclusion Chromatography. The effects of protein concentration, pH, and KCl concentration on the oligomerization of Fur were monitored by analytical size exclusion chromatography (Superdex 75 10/30 Amersham Biosciences) using a FPLC system at a flow rate of 1 mL/min at 4 °C. The relative amount of each oligomer was measured by integration of the area under the curve (absorbance at 280 nm) using GraphPad Prism and a Gaussian model to resolve overlapping peaks. The data were then analyzed according to a method derived from Manning et al. (*27*) to obtain the equilibrium constant for tetramer dissociation, K_{tet} (see the Supporting Information). The molecular masses were estimated using a molecular mass calibration kit (Amersham Biosciences). The protein solutions to be analyzed were prepared as described below.

Influence of Protein Concentration. A solution of the dimer (Zn_1Fur_D) in 0.1 M MOPS (pH 7.5), containing 0.1 M KCl, was concentrated to 3 mM using Ultrafree 0.5 (Millipore) and was diluted to 1.5, 1.0, 0.5, and 0.2 mM with MOPS buffer. The solutions were allowed to equilibrate for 6 h at 25 °C.

Influence of KCl Concentration. Three samples were prepared at various KCl concentrations. A solution of concentrated Zn_1Fur_D [3 mM in 0.1 M MOPS (pH 7.5) and 0.1 M KCl] was diluted twice in 0.1 M MOPS (pH 7.5) containing 0.1, 1, and 2 M KCl. The three solutions were allowed to equilibrate for 6 h at 25 °C.

Influence of pH. Solutions of Fur (Zn_1Fur_D) at pH 6.5, 7.0, 8.0, and 9.0 were prepared from the same stock solution of the dimer. Samples of the stock solution [500 μL, 250 μM in 0.1 M Tris-HCl (pH 8) containing 0.1 M KCl] were loaded on a Sephadex G-25 column (Amersham Biosciences) equilibrated with 0.1 M Bis-Tris propane (pH 6.5, 7, 8, or 9) containing 0.1 M KCl. Various protein concentrations (240, 180, 120, 60, and 20 μM) were obtained by dilution of the resulting solutions (500 μL, 250 μM) in the corresponding buffer, and the final solutions were allowed to equilibrate for 10 h at 4 °C.

Monomer to Dimer Conversion. To avoid artifactual effects caused by metal contamination, high protein concentrations were used in these experiments, but the same behavior was observed at 10 μM. The monomer at 1.9 mM in 0.1 M Tris-HCl (pH 8) containing 0.1 M KCl was incubated in the presence of DTT and/or $ZnSO_4$ at 25 °C for 10 min or 1 h before being loaded onto the column equilibrated with the same buffer.

Oxidation State of Thiols in the Monomer. Alkylation of the thiol groups of the monomer was performed as previously described for the dimer (*23*). The purified dimer (Zn_1Fur_D) (50 μM) and the monomer (50 μM) in 0.1 M Tris-HCl (pH 8) 0.1 M KCl, and 50 mM EDTA were treated with freshly prepared iodoacetamide (6 mM) for 24 h. The proteins were then desalted using a C_4 ZipTip column (Millipore) in 10 mM ammonium acetate buffer and analyzed by electrospray

mass spectrometry. Endoproteinase Lys-C digestions were performed with 1% (w/w) endoproteinase Lys-C for 6 h in 100 mM ammonium bicarbonate buffer at pH 7.9 on a 25 μM monomer sample before MALDI analysis.

EDC Cross-Linking. A fresh solution of EDC was prepared each time (in the same buffer), and the incubations with EDC were performed at room temperature in the dark. The purified monomer (Fur_M) and dimer (Zn_1Fur_D) samples (40 μM) were incubated in 20 mM MOPS (pH 7) containing 150 mM KCl, in the presence of 10 equiv/subunit DTT, 100 equiv/subunit EDTA, and various numbers of equivalents per subunit of metal ion sulfate (1, 10, and 100) as indicated in Figure 4. After incubation for 5 min with above-mentioned reagents, the sample was either treated with EDC without buffer exchange (Figure 4B, lanes 6−10) or exchanged (Microbiospin, Bio-Rad) with 20 mM MES buffer (pH 6.5) containing 150 mM KCl (Figure 4A, lanes 2−9, and Figure 4B, lanes 2−5) and subsequently incubated for 1 h with 20 mM EDC. The yield of the cross-link was estimated by SDS−PAGE in the presence of β-mercaptoethanol. Concentrations of reagent and protein were chosen to produce a yield of cross-linked dimer reaching roughly 40−50% of total protein. For mass analyses, the reaction was performed in 20 mM Mes (pH 6.5) and 150 mM KCl and the reagent was removed by dialysis after the incubation, and the protein was then treated with hydroxylamine, to hydrolyze the *O*-acyl isourea groups resulting from the fixation of EDC on unreacted carboxylates (*28*−*30*). Cross-linked dimer and unreacted monomers were separated using reversed phase HPLC on a C4 Brownlee column (2.1 mm × 150 mm, Applied Biosystems). Solvent A was a solution of 0.1% trifluoroacetic acid in water, and solvent B was a 90/10/0.08 acetonitrile/water/trifluoroacetic acid mixture. The column was equilibrated in 10% solvent B, and the species were separated with a slow gradient of solvent B in A (from 10 to 40% over 30 min and then from 40 to 55% over 15 min).

Analysis of Peptides Cross-Linked with EDC. In each case, the covalent dimer obtained after the reaction with EDC was separated from nonlinked monomers by HPLC, allowing measurement of the cross-linking yield (data not shown).

Fractions containing the cross-linked dimer were dried with a Speed-vac concentrator and dissolved in 100 mM ammonium acetate (pH 7.5) for proteolytic cleavage. Approximately 1% (w/w) endoproteinase Lys-C was added to each of them, and the mixture was incubated at 37 °C overnight. Resulting peptides were analyzed by MALDI-TOF-MS. For further characterization of the cross-linking site, peptides were separated by reversed phase HPLC on a C18 Brownlee column (1 mm × 150 mm, Applied Biosystems). Solvents A and B were the same as described above. The following gradient was used: from 0 to 30% solvent B over 100 min and then from 30 to 80% over 40 min. Fractions were analyzed by MALDI-TOF mass spectrometry, and the fractions containing the cross-linked peptides were dried and dissolved in 100 mM ammonium acetate (pH 7.5) for further cleavage of the C-terminal peptide with chymotrypsin. Approximately 1% (w/w) enzyme was added, and the mixture was incubated for 6 h at 37 °C. Resulting peptides were separated using the following gradient: from 2 to 32% solvent B over 70 min and then from 32 to 82% solvent B over 30 min. After MALDI-TOF-MS analysis of the fractions, one of them was shown to contain the digested cross-linked peptides and was thus treated with cyanogen bromide for further cleavage after the methionine of the N-terminal peptide. The fraction was dried and then dissolved in 70 μL of pure TFA before addition of 30 μL of water and 1 mg of cyanogen bromide. The mixture was incubated overnight at 5 °C, then dried, dissolved in water, and analyzed by MALDI-TOF-MS.

DMA Cross-Linking. The reaction was performed in 200 mM triethanolamine buffer (pH 8.5), at a protein concentration of 60 μM. Dimethyl apimidate was freshly prepared in the same buffer and added to a final concentration of 50 mM. The mixtures were incubated for 30 min at room temperature and then immediately frozen in liquid nitrogen. For the Mn-containing dimer, 200 μM Zn_1Fur_D was incubated with 2 mM $MnCl_2$ for 15 min at 37 °C and then diluted 10-fold in 50 mM triethanolamine buffer (pH 8.5). Purification and separation of the monomer and cross-linked dimer were performed by reversed phase HPLC as described in the case of EDC cross-linking.

Analysis of Peptides after Treatment with DMA. Fractions containing the monomer or the cross-linked dimer were dried and redissolved in 100 mM ammonium acetate buffer (pH 7.5) for proteolytic cleavage. Approximately 1% (w/w) endoproteinase Glu-C was added, and the mixture was incubated at 25 °C overnight. Resulting peptides were separated by HPLC on a C18 reversed phase column (1 mm × 150 mm, Applied Biosystems). Solvent A and solvent B were the same as previously described. A gradient from 0 to 60% solvent B over 60 min was used. For detection of cross-linked peptides, fractions were analyzed by MALDI-MS.

Mass Spectrometry Analysis. Electrospray mass spectrometry of peptides and proteins was performed using a SCIEX API III+ triple-quadrupole mass spectrometer (Perkin-Elmer Sciex) equipped with a nebulizer-assisted electrospray source. Poly(propylene glycol) ions were used for calibration in the positive mode. The ion spray voltage was set at 5000 V, the orifice voltage at 80 V, and the interface temperature at 55 °C. Measurement of dimeric and oligomeric species was performed with an electrospray TOF (time-of-flight) mass spectrometer (Micromass, Manchester, U.K.), under nondenaturing conditions. MALDI-TOF mass spectrometry of peptides was performed on a Perseptive Voyager XL (Perseptive Biosystems) time-of-flight mass spectrometer. A solution of 2,5-dihydrobenzoic acid in a water/acetonitrile/TFA mixture (50/50/0.1) was used as the matrix. A volume of 1 μL of crude peptide mixture was mixed on the target with an equal volume of matrix, and the drop was allowed to air-dry. Spectra were acquired in linear mode.

DNA Binding Monitored by Fluorescence Anisotropy. Site specific DNA binding of oxidized monomeric Fur (Fur_M^{SS}) and dimeric Fur (Zn_1Fur_D) was assessed using fluorescence anisotropy. 5′-Fluorescein-labeled single-strand DNA (Fl-5′-gggGATAATGATAATCATTATCggg-3′) and its nonlabeled complementary strand were purchased from Sigma Genosys. Both strands were annealed using standard methods (*31*), and the presence of at least 90% duplex DNA was confirmed by PAGE. The change in fluorescence anisotropy of the labeled DNA upon binding of Fur species was followed using a thermostated Perkin-Elmer LS50B fluorimeter, with the manufacturer's modifications for fluores-

cence polarization measurements. The settings for optimal fluorescence yield were used as follows: excitation at 494 nm (2.5 nm slit) and emission at 527 nm (20 nm slit) with a 515 nm cutoff filter. The *g* factor was regularly checked and was always very close to 1.00, and this value was thus used in all anisotropy calculations (using the manufacturer's software). The fluorescence yield of the duplex was not significantly affected during the Fur titrations. Measurements were performed at 25 °C using a 1 cm × 1 cm, 3 mL stirred cell. Routinely, 2.2 mL of 10 nM labeled DNA was used, in 20 mM MOPS (pH 7) and 150 mM KCl, and in the presence of 10 μg/mL poly(dIdC) (Amersham Biosciences) and 12 mM $MgSO_4$ to exclude nonspecific binding. In some of the experiments, 1 mM $MnSO_4$ was present, to activate Fur for DNA binding. Binding curves were analyzed using the Hill equation:

$$r = r_0 + \Delta r \frac{[\mathrm{Fur}]^n}{{K_{1/2}}^n + [\mathrm{Fur}]^n} \quad (1)$$

where r represents the anisotropy of the DNA, r_0 the anisotropy of unbound DNA, and Δr the change in anisotropy upon binding. $K_{1/2}$ is where 50% of the DNA is bound, and n is the Hill coefficient, a factor that represents the cooperativity of binding.

CD Spectroscopy. Far-UV CD spectra (190−250 nm) of the oxidized monomer (Fur_M^{SS}), the reduced monomer (Fur_M^{SH}), the reduced monomer titrated with 0.3−1.3 equiv of zinc, and the dimer (Zn_1Fur_D) were recorded on a Jasco J-810 spectropolarimeter at 25 °C. A 1 mm path length cell was used for the measurement, and the parameters were set as follows: bandwidth, 4 mm; step resolution, 0.5 mm; scan speed, 100 nm/min; and response time, 2 s. Each spectrum was obtained as the average of four scans. The protein concentration was typically around 20 μM. Prior to the calculation of the mean residue molar ellipticity, all of the spectra were corrected by subtracting buffer contributions.

Dimer to Monomer Conversion. Samples of dimeric Fur (Zn_1Fur_D) at 20 μM in 0.1 M Tris-HCl (pH 8) containing 0.5 M KCl were incubated at 25 °C while being stirred in the presence of 2 mM oxidative reagent (H_2O_2 or diamide). The effect of a concomitant addition of EDTA at 2 mM was also checked. Aliquots were taken after various times of incubation (0 and 30 min and 1, 3, 6, and 24 h) and subsequently analyzed by analytical size exclusion chromatography. The data were analyzed with GraphPad Prism assuming a pseudo-first-order reaction rate (with H_2O_2 concentration raised constant).

RESULTS

Oligomerization Studies. The Fur protein appears to exist mainly as a dimer in solution as previously shown from HPLC studies (*12*) and mass spectrometry (*13*). Nevertheless, we observed by size exclusion chromatography (Figure 1) and mass spectrometry (Figure 2) that the dimeric form is involved in several oligomeric equilibria depending on protein concentration, KCl concentration, and pH. The chromatograms presented in Figure 1A display species eluting at 10.3, 8.9, and 8.3 mL associated with molecular masses of 39, 66, and 87 kDa and consistent with dimeric, tetrameric, and hexameric species, respectively. The proportion of higher oligomers increases as a function of the protein concentration (Figure 1A). When the fractions containing the tetramer and the hexamer were collected, concentrated, and re-injected onto the same column, a substantial amount of dimer was eluted, indicating that oligomerization of the dimer is reversible (not shown). Mass spectrometry measurements performed under soft nondenaturing conditions showed a major form corresponding to a dimer, plus other peaks that could only be ascribed to tetrameric (T17+ and T15+) and hexameric (H22+, H20+, H19+, and H18+) species (Figure 2A), in agreement with the results of size exclusion chromatography. The exact mass calculated for the dimeric form was consistent with the presence of two zinc atoms per dimer (Figure 2B). As previously reported, the purified dimer contains one zinc ion per monomer, coordinated in a high-affinity site, and Zn_1Fur_D will refer to this form later in the text (*13*, *21*).

When the concentration of KCl was increased, the oligomerization equilibrium was shifted in favor of the dimer, even at high protein concentration such as 1.5 mM (Figure 1B). Fur was eluted mainly as a dimer at pH 9.0, 8.0 (not shown), and 7.0 (Figure 1C). In contrast, oligomerization was enhanced when the pH was decreased below 7.0 (Figure 1C,D). The equilibrium constant for the dimer−tetramer equilibrium was determined according to the method of Manning et al. (*27*) but modified to take into account the equilibrium between tetramer and higher oligomers (Figure 1E). Equilibrium constants for tetramer dissociation of 0.72 ± 0.02 and 5.0 ± 0.1 mM at pH 6.5 and 7, respectively, were obtained at 4 °C in 0.1 M BTP and 0.1 M KCl (Figure 1E).

Another species eluted at 11.3 mL, corresponding to a monomeric species (apparent molecular mass of 23 kDa), appeared after a relative long incubation time. A monomeric species is also usually co-isolated during Fur purification (see Experimental Procedures). When the monomer-containing fractions were collected, concentrated, and re-injected onto the gel filtration column, a single elution peak at 11.3 mL was obtained (data not shown), indicating that the as-isolated monomer is not in equilibrium with the dimer as described above for the oligomerization of the dimer (*13*).

Oxidation State of Thiols in the As-Isolated Monomeric Form. We had already noticed that the presence of excess amounts of EDTA (100 mM in place of 20 mM) during Fur purification leads to an increased percentage of monomeric Fur (not shown). This suggested the involvement of a metal site in the dimerization process. In the dimeric form of *E. coli* Fur (Zn_1Fur_D), the zinc ion coordinates cysteines 92 and 95 by their sulfur atom and cysteines 132 and 137 were reduced (*23*). The free thiol content of the monomer was analyzed by cysteine alkylation using iodoacetamide under nondenaturing conditions and mass spectrometry analyses [as previously described for the dimer (*23*)]. The results were compared to those obtained for the dimer (Zn_1Fur_D) in the presence of EDTA, which was shown to accelerate the alkylation of C92 and C95. Alkylation of all four cysteines in the dimer demonstrated that the cysteines were not oxidized in dimeric Fur. In contrast, none of the cysteines in the monomer reacted with iodoacetamide. On this form, alkylation of the four cysteines could only be achieved in the presence of DTT. These results indicate that all four

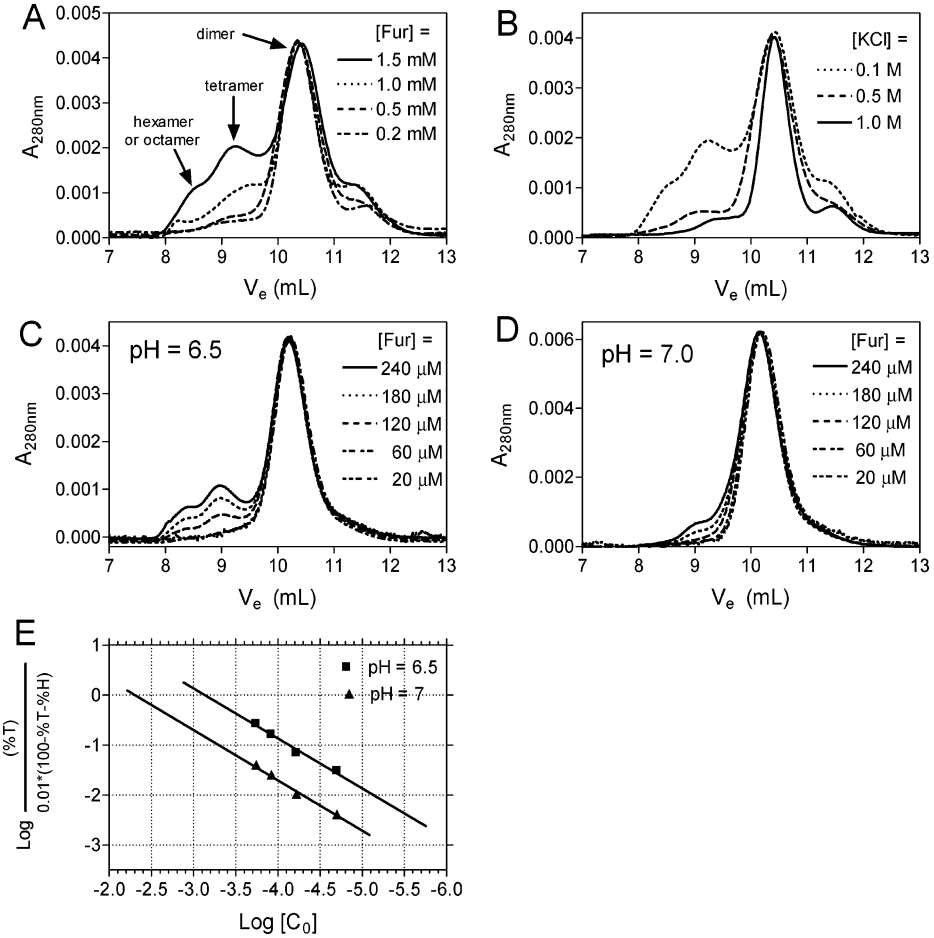

FIGURE 1: Influence of protein concentration, KCl concentration, and pH on the oligomerization equilibrium, followed by size exclusion chromatography. Chromatograms of Fur at various protein concentrations (A), various KCl concentrations (B), and various protein concentrations at pH 6.5 (C) and 7.0 (D). The protein concentrations, expressed in subunit concentration, were (A) 1.5, 1.0, 0.5, and 0.2 mM in 0.1 M MOPS and 0.1 M KCl (pH 7.5) (solutions allowed to equilibrate for 6 h at 25 °C), (B) 1.5 mM in 0.1 M MOPS (pH 7.5) containing KCl at 0.1, 0.5, and 1 M (solutions allowed to equilibrate for 6 h at 25 °C), and (C and D) 240, 180, 120, 60, and 20 μM in 0.1 M BTP and 0.1 M KCl [pH 6.5 (C) and 7.0 (D)] (solutions allowed to equilibrate for 10 h at 4 °C). All these solutions were loaded on a Superdex 75 HR 10/30 column (Amersham Biosciences) equilibrated with the corresponding buffer. Final protein and KCl concentrations are given. All the chromatograms were normalized to the peak of the dimer. (E) Plot according to Manning et al. (*27*) of log(C_0) vs log{(%T)/[0.01(100 − %T − %H)^2]}, where C_0 represents the total protein concentration and %T and %H represent the percentages of tetramer and hexamer, respectively (protein concentrations expressed in monomeric subunit concentration). A linear fit through the data points with a slope of 1.0 gives the equilibrium constants at $y = 0$. In our case, the equilibrium constants were 0.72 ± 0.02 and 5.0 ± 0.1 mM at pH 6.5 and 7, respectively, in 0.1 M BTP and 0.1 M KCl at 4 °C.

cysteines were oxidized in the purified monomeric species (Table 1S of the Supporting Information).

Subsequently, the monomer was digested with endoproteinase Lys-C, and the peptides were analyzed using MALDI mass spectrometry to identify the modification of the cysteines. Two distinct peptides, bearing C92 and C95 (fragment of residues 78−98) on one hand and C132 and C137 (fragment of residues 118−148) on the other hand, were identified, and no peak corresponding to cross-linked fragments (residues 78−98 and 118−148) was detected, showing that no disulfide bridge was formed between either cysteine of these two groups (Table 2S of the Supporting Information). Both peptides had a molecular mass 2 Da lower than that expected from the peptide sequence. After incubation of the monomer with DTT, the mass was exactly as expected (Table 2S of the Supporting Information). This indicates that the oxidized monomer digested by endoproteinase Lys-C contains two disulfide bridges, one between C92 and C95 and another one between C132 and C137. It has to be noticed that a mass deviation of 2 Da was also measured in the peptide containing C132 and C137 after digestion of the dimeric species, Zn_1Fur_D (see Cross-Link Experiments), although in this species these residues are not initially oxidized. Therefore, by itself, this mass deviation is not indicative of a disulfide bond in the protein as it can be attributed to oxidation under the conditions used for enzymatic digestion. However, alkylation experiments with iodoacetamide, performed with the native protein itself, clearly show that the cysteine residues in the monomeric species are completely unavailable for reaction. Altogether, these data indicate the presence of two disulfide bridges in the as-isolated monomer and will be denoted Fur_M^{SS} later in the text.

Monomer to Dimer Conversion. The monomer and dimer are not in a simple equilibrium as mentioned above. However, having shown that the sulfur atoms that are normally bound to the zinc ions are involved in a disulfide bridge in the monomer, we assessed the effect of reductant (DTT) and zinc ions on the oligomeric structure of the monomer (Fur_M^{SS}). Figure 3 shows chromatograms obtained

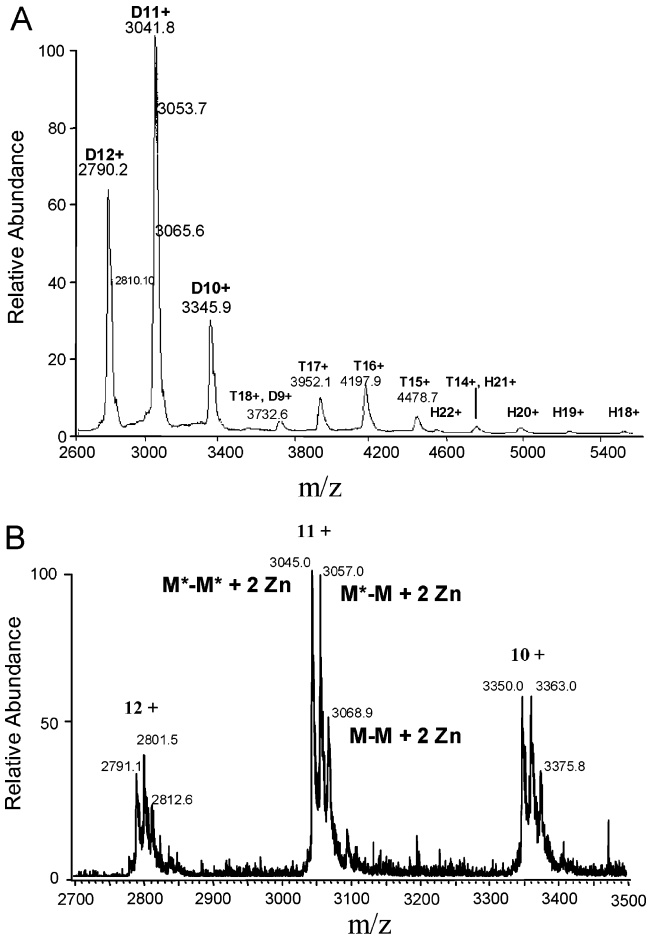

FIGURE 2: Identification of oligomers by mass spectrometry under nondenaturing conditions. (A) Mass spectrum of Fur under nondenaturing conditions indicating the presence of oligomeric states. Peaks corresponding to the dimeric, tetrameric, and hexameric forms have been labeled D, T, and H, respectively, with the associated state of charge. The protein sample (100 μM in ammonium acetate buffer at pH 6.6) was injected using nanospray in an electrospray TOF mass spectrometer. (B) Expansion of the *m*/*z* range from 2700 to 3600. M symbolizes a monomer unit, the asterisk the N-terminal methionine-excised form, and Zn the zinc ion content.

after treatment of the monomer with DTT and addition of a stoichiometric amount of zinc. We observed that addition of zinc and DTT leads to formation of dimer in <10 min (Figure 3A). Interestingly, this process was faster when DTT was added first than when zinc was added first (data not shown). When zinc ion was added 1 h after addition of DTT, the yield in dimer was decreased by approximately 50% (Figure 3B) compared to a situation in which it was added only 10 min after DTT. In contrast, neither reduction of the thiolates (Figure 3C) nor addition of a stoichiometric amount of zinc alone (Figure 3D) leads to dimerization. The addition of other dications, such as Co^{2+} or Mn^{2+}, instead of zinc, also led to the formation of a dimer in the presence of DTT (data not shown).

Cross-Link Experiments. Cross-linking reactions have been widely used to study protein−protein interactions and to prove interaction or proximity between several protein components in a complex (*28*−*30*).

Cross-Linking with Ethylene Carbodiimide. Ethylene carbodiimide (EDC) is a "zero-length cross-linker" creating a covalent link between a carboxylate and an amine in an ionic interaction (*28*−*30*). EDC-treated Fur dimer (Zn_1Fur_D)

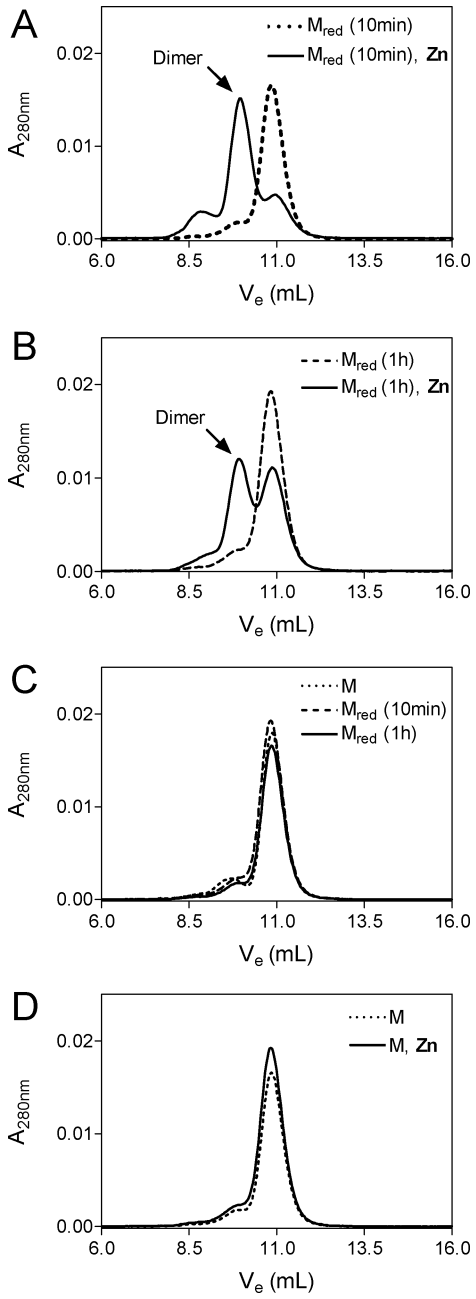

FIGURE 3: Influence of DTT and zinc on monomer, followed by size exclusion chromatography. Size exclusion chromatography profile of the monomeric species at 1.9 mM in 0.1 M Tris-HCl buffer (pH 8) containing 0.1 M KCl in the presence of DTT and/or Zn^{2+} at 25 °C. (A) Ten minutes after addition of 4 equiv of DTT/monomer, 1 equiv of Zn^{2+}/monomer was added. (B) One hour after addition of 4 equiv of DTT/monomer, 1 equiv of Zn^{2+}/monomer was added. (C) After addition of 1 equiv Zn^{2+}/monomer. (D) After addition of 4 equiv of DTT/monomer.

samples gave a clear band in SDS−PAGE corresponding to a species with a molecular mass of 34 kDa on the gel in addition to the 17 kDa band normally observed for denatured Fur, indicating that the major reaction product was actually a cross-linked dimer (Figure 4B, lane 2). DTT and EDTA have no effect on the yield of the EDC cross-link with the dimer (Figure 4B, lanes 3−5). In contrast, no 34 kDa band was observed after EDC treatment of the monomer, Fur_M^{SS} (Figure 4A, lane 2). When monomer (Fur_M^{SS}) samples were pretreated with DTT and/or zinc, we clearly observed the cross-linked dimer 34 kDa band (Figure 4A, lanes 5 and 6).

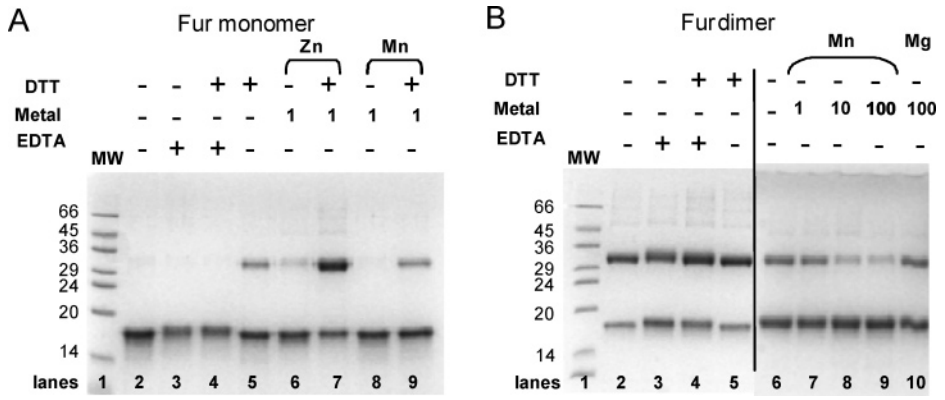

FIGURE 4: Influence of DTT, Zn^{2+}, and Mn^{2+} on monomer, followed by EDC cross-linking. SDS−PAGE analysis of the EDC cross-link experiment of Fur monomer (A) and dimer (B). The Fur monomer and dimer samples [40 μM in 20 mM MOPS buffer (pH 7) containing 0.15 M KCl] were incubated in the presence of 10 equiv of DTT/subunit, 100 equiv of EDTA/subunit, and various numbers of equivalents per subunit of the metal ion sulfate (1, 10, and 100) as indicated. The EDC treatments were performed as described in Experimental Procedures.

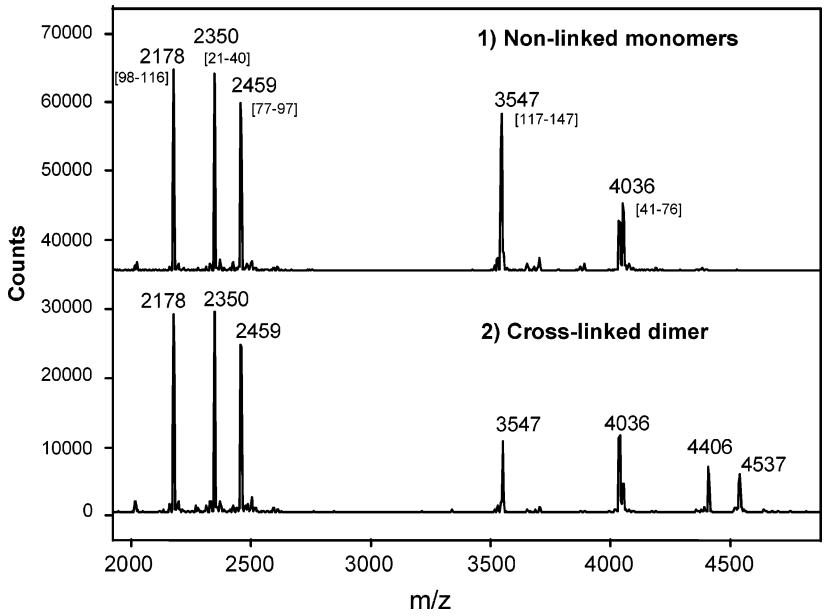

FIGURE 5: MALDI-TOF mass spectra of the digested cross-linked dimer. MALDI-TOF mass spectra of peptide mixtures obtained by endoproteinase Lys-C digestion of (1) nonlinked monomers and (2) covalent cross-linked dimer, isolated after treatment of the protein with EDC. A mass deviation of 2 Da from the theoretical value of *m*/*z* 3549 was observed for this peptide and can be attributed to formation of a disulfide bridge between cysteines C132 and C137 under the conditions used for enzymatic digestion.

Pretreatment with both reagents simultaneously, DTT and zinc, appeared to be most efficient (Figure 4A, lane 7). When EDTA was added to the reaction mixture with DTT only, the cross-linked species was not observed, indicating that some metal contaminants in our solutions may play the role of the zinc ions (Figure 4A, lanes 3 and 4). It is likely that the cross-linking observed in the absence of added DTT (Figure 4A, lane 5) is caused by the presence of some reduced monomer (Fur_M^{SH}) in the samples. When Mn^{2+} was used instead of Zn^{2+} to generate Mn_1Fur_D (Figure 4A, lanes 8 and 9), formation of the cross-linked species was also observed in the presence of DTT, but the yield was much lower. When manganese ions were added to the dimeric form (Zn_1Fur_D) to generate the activated dimer ($Zn_1Mn_2Fur_D$), the yield of cross-link was drastically decreased for [Mn^{2+}]/[Fur] ratios of 10 and 100 (Figure 4B, lanes 6−9). In the same proportion, Mg^{2+} [unable to activate the Fur protein (*7*)] does not alter the yield of the cross-link (Figure 4B, lane 10). According to the different values of the dissociation constant reported in the literature for the manganese in the regulatory site, $K_d(Mn^{2+}/Fur)$ [20 (*32*), 80 (*33*), and 85 μM (*34*)], between 20 and 50% of the dimeric protein would be loaded with Mn^{2+} for a ratio of 1 and 85−100% for ratios of >10. These results suggest that the intersubunit ionic interaction, targeted by the EDC cross-link, is lost upon metal binding.

To identify the amino acids involved in the cross-link, the dimer Zn_1Fur_D was successively digested. The cross-linked and non-cross-linked species were purified and digested with endoproteinase Lys-C, and the crude peptide mixture was analyzed using MALDI-TOF-MS (Figure 5). Interestingly, new peaks at *m*/*z* 4406 and 4537 appeared in the peptide map of the cross-linked dimer. These masses were consistent with species comprising the C-terminal peptide, H117−K147, of one monomer linked to the N-terminal peptide of the other monomer. Furthermore, the intensity of the peak at *m*/*z* 3547, corresponding to the free form of H117−K147, was reduced in the peptide map of the cross-linked dimer, in agreement with H117−K147 being involved in a cross-

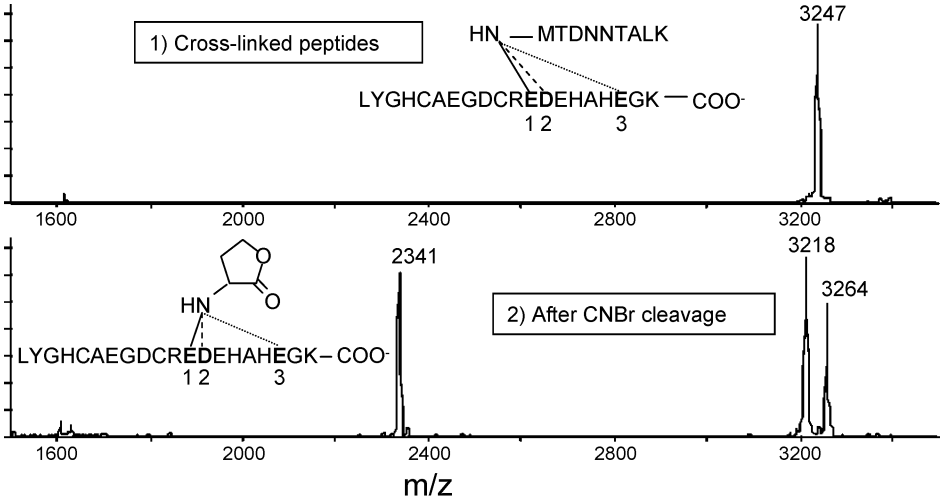

FIGURE 6: Identification of amino acids linked with EDC. MALDI-TOF mass spectra were obtained for (1) cross-linked peptides (MT1−K8 and H117−K147) after chymotrypsin digestion and (2) resulting peptides after CNBr cleavage.

link. Two signals were detected for the cross-linked peptides, with a mass difference of 131 Da, corresponding to the N-terminal methionine that is incompletely processed during overexpression (*13*). Therefore, the cross-linked N-terminal peptide corresponds to T1−K8 and MT1−K8.

The cross-linked peptides were subsequently purified and digested with chymotrypsin (Figure 6-1). We found that the peptide of residues L128−K147 and not H117−Y127 was cross-linked to T1−K8 and to MT1−K8. Edman degradation of both species gave a sequence in which amino acids E139, D140, and E145 were missing from the L128−K147 moiety, suggesting that one or several of these residues were involved in the cross-link. No sequence was obtained for T1−K8 and MT1−K8, indicating that the N-terminal NH_2 group of this moiety was not available and thus probably involved in the cross-link. The peptide corresponding to L128−K147 cross-linked to MT1−K8 was treated with CNBr to allow cleavage after the methionine (Figure 6-2). Mass determination of the resulting peptide by MALDI-MS gave a peak at *m*/*z* 2341, consistent with the L128−K147 peptide still linked to the N-terminal methionine, after release of T1−K8. This confirmed that the cross-link existed between the N-terminal NH_2 group of one monomer and one of the glutamate or aspartate residues (E139, D140, and E145) located in the C-terminal end of the other monomer.

Cross-Linking with Imidoesters. DMA is a homobifunctional imidoester that specifically reacts with primary amine groups (i.e., ϵ-amino groups of lysine residues, the N-terminal amine of the backbone) and cross-links two primary amine groups located <8.6 Å from each other. After reaction of the protein with DMA, cross-linked and non-cross-linked species were purified and digested with endoproteinase Glu-C. Some peptide appears specifically from the digestion of the cross-linked species. MALDI-TOF-MS analyses gave peaks at *m*/*z* 3368, consistent with a cross-link occurring between the N-terminal T1−E23 peptide of one monomer and G74−E80 peptide of the other monomer. Another peptide gave a signal at *m*/*z* 4988 that is consistent with a cross-link between the N-terminal T1−E23 peptide of one monomer and the L81−E100 peptide of the other monomer. Both peptides, L81−E100 and G74−E80, include a single lysine, K76 and K97, respectively, each of which is a potential target of the DMA cross-linker. Therefore, K76 and K97 of one monomer seem to be located <8.6 Å from one or several amino groups of the N-terminal part of the other monomer.

Furthermore, when DMA was added on the metal-activated manganese-bound Fur ($Zn_1Mn_2Fur_D$), we observed that the yield of the DMA cross-link of the dimer decreased by almost 50%. This suggests that binding of metal to the dimer in the regulatory site causes an increase in the distance between the amino acids of each monomer involved in this cross-link.

Secondary Structure Changes Followed by Circular Dichroism. The results presented in Figure 7 show that addition of DTT does not affect the secondary structure of Fur_M^{SS}, indicating no major secondary structural changes take place upon reduction of the cysteine. Addition of zinc to the reduced monomer, Fur_M^{SH}, quantitatively results in formation of a species indistinguishable in secondary structure from the dimer, Zn_1Fur_D (Figure 7A and inset). CD spectroscopy confirmed that both zinc and DTT were required for dimerization from the oxidized monomer, Fur_M^{SS}. This result further indicates that the reconstituted dimer exhibits the same secondary structures as the purified dimer, Zn_1Fur_D. The CD spectra of monomeric species (Fur_M^{SH} and Fur_M^{SS}) and dimeric Fur (Zn_1Fur_D) indicate a mixed α-helix and β-sheet secondary structure with a significant degree of α-helical structure, in agreement with the *P. aeruginosa* Fur dimer structure (42% of α-helices) (*18*). The difference spectrum of the Zn_1Fur_D dimer and Fur_M^{SS} (Figure 7B) indicates a change in secondary structure composition upon dimerization of Fur. The decrease in negative ellipticity between 200 and 207 nm, and around 227 nm, most likely indicates a relative increase in the fraction of β-sheet over α-helix upon dimerization. The difference in ellipticity between both types of secondary structure is largest in these wavelength regions. However, the change in the 220−240 nm region could also be associated with a change in the environment near aromatic residues, especially tyrosine (*35*, *36*).

DNA Binding Activity of Monomeric and Dimeric Fur. The DNA binding activities of Fur dimer (Zn_1Fur_D) and oxidized monomer (Fur_M^{SS}) were determined by fluorescence

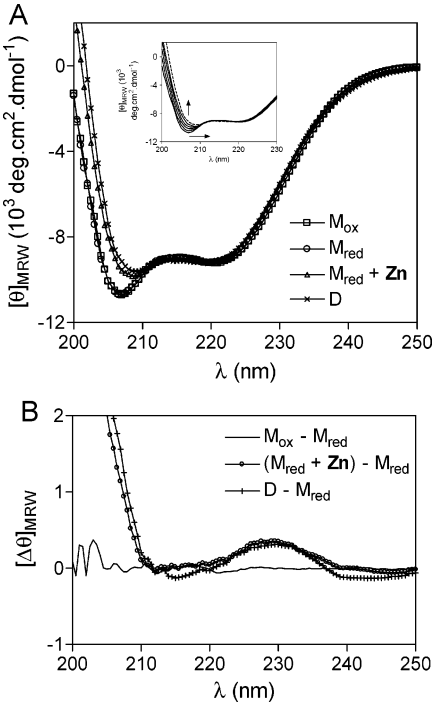

FIGURE 7: Circular dichroism spectra of *E. coli* Fur at 20 μM in the far UV. (A) Fur dimer (D) compared to the oxidized monomer (M_{ox}) and the reduced monomer (M_{red}) obtained after addition of 20 equiv of DTT/monomer and the reduced monomer plus one zinc sulfate equivalent per monomer (M_{red} + Zn). The inset shows zinc titration of the reduced monomer after addition of 0.3, 0.6, 0.9, and 1.2 equiv of Zn^{2+}/monomer. (B) M_{ox} − M_{red}, (M_{red}+Zn) − M_{red}, and D − M_{ox} difference spectra. The buffer contribution [20 mM MOPS and 40 mM KCl (pH 7)] was always subtracted from the spectra which were all normalized with respect to the protein concentration.

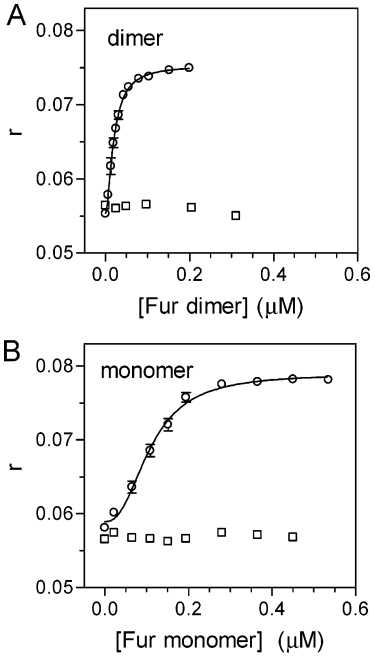

FIGURE 8: DNA binding activity followed by fluorescence anisotropy. The DNA binding was followed by a fluorescence anisotropy experiment with the dimer and monomer to a 25 bp fluorescein-labeled oligonucleotide containing the consensus Fur box in the absence (□) and presence (○) of 1 mM $MnSO_4$ in the buffer. The anisotropy is plotted as a function of total protein concentration. The solid lines through the data represent fits with GraphPad Prism using the Hill equation (see the text). Conditions: 10 nM DNA in 20 mM MOPS buffer (pH 7) containing 150 mM KCl, 10 μg/mL poly(dIdC), and 12 mM $MgSO_4$ at 25 °C.

anisotropy using a 25 bp fluorescein-labeled oligonucleotide containing the 19 bp consensus Fur box sequence [the most simple motif known to undergo in vivo regulation (*6*)]. Three GC base pairs were added on both sides of the Fur box to improve the duplex stability and prevent hairpin formation. DNA binding of Zn_1Fur_D and Fur_M^{SS} was clearly observed only in the presence of Mn^{2+} (1 mM $MnSO_4$) (Figure 8). Addition of excess EDTA to Mn^{2+}-containing solutions led to an immediate lowering of the fluorescence anisotropy to the initial value for both Zn_1Fur_D and Fur_M^{SS} (not shown). In all cases, the titrations were performed in the presence of excess (10 μg/μL), unlabeled poly(dIdC), thus excluding nonspecific DNA binding as the origin of the anisotropy increase.

Fitting of the binding curves using discrete models (1:1, 1:2, sequential, and pre-association) does not give satisfactory fitting. The affinity of Fur for manganese is weaker for the monomer than for the dimer (unpublished data), but a fit for these data is beyond the scope of the work presented here. Then, the Hill equation was used expressly to compare dimer and monomer apparent binding constants, or binding midpoints. The binding curves of Zn_1Fur_D and Fur_M^{SS} in the presence of Mn^{2+} were fitted using the Hill equation, yielding the following values for the binding midpoint and Hill constant: $K_{1/2} = 20 \pm 1$ nM and $n = 1.66 \pm 0.07$ for Zn_1-Fur_D and $K_{1/2} = 109 \pm 2$ nM and $n = 2.40 \pm 0.1$ for Fur_M^{SS}. It was surprising to us that the oxidized monomer was able to bind specifically to the DNA. We were therefore especially careful to exclude the presence of traces of dimeric Fur. Dimeric Fur could also arise from contamination by reduced monomer Fur_M^{SH}, which will dimerize upon addition of Mn^{2+}. Using exclusion chromatography with 1 mM $MnSO_4$, both after and before the titration, neither Fur dimer nor reduced monomer able to dimerize under the experimental conditions could be detected.

Dimer to Monomer Transition. The dimer, Zn_1Fur_D, was treated with diamide (an oxidant of thiol) and hydrogen peroxide. The reaction was monitored by size exclusion chromatography. When hydrogen peroxide or diamide was added, two new species appeared, eluted at 11.3 and 13 mL, corresponding to a monomeric species and probably to degraded protein. Figure 9 shows the evolution of proportions of dimer, monomer, and degraded species as a function of time after H_2O_2 treatment. The decrease in dimer concentration was correlated to the appearance of the monomer and the degraded species. The rate of dimer disappearance was analyzed using a pseudo-first-order reaction rate, yielding a pseudo-first-order reaction rate constant, with 2 mM H_2O_2 and a k of 0.28 ± 0.02 h^{-1} ($t_{1/2} = 2.5$ h). Similar results were obtained with diamide, but exhibiting a slower rate ($k = 0.14 \pm 0.01$ h^{-1}). The addition of 2 mM EDTA by itself did not lead to formation of a monomer on this time scale (24 h), but it did accelerate the formation of the monomer when added together with diamide ($k = 0.20 \pm 0.01$ h^{-1}).

DISCUSSION

This paper describes the various oligomeric states of Fur and the factors involved in their interconversion. Scheme 1 summarizes these results. It is possible that in vivo Fur exists in oligomeric states other than the well-characterized dimeric

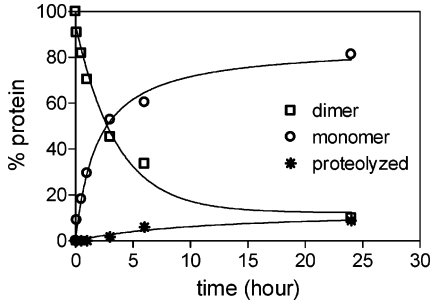

FIGURE 9: Influence of H_2O_2 on the dimeric form. Evolution in time of the percentage of the dimer, monomer, and proteolyzed forms after treatment of 20 μM Fur dimer with 2 mM H_2O_2. The concentration of each species was determined using size exclusion chromatography by measuring the area under the peak of each species. The pseudo-first-order rate constant for dimer disappearance (k'), with 2 mM H_2O_2, was 0.28(2) h^{-1} ($t_{1/2}$ = 2.5 h).

state. This may be a consequence for the tuning of Fur regulation.

Oligomerization Properties of Dimeric Fur. Size exclusion chromatography and mass spectrometry analysis clearly show the presence of tetramer and higher-molecular mass species. We show that oligomerization is sensitive to pH and salt concentration. The decreased tendency to oligomerize at high KCl concentrations suggests that oligomerization is due to intersubunit salt bridges, as these will be less effective at higher ionic strengths. A decrease in the pH favors formation of higher-order oligomers. The equilibrium constant of dissociation of the tetramer decreases 7-fold when the pH is decreased from 7 to 6.5. This is consistent with earlier electron microscopy studies indicating a pH-driven oligomerization: tetramer and higher oligomeric states were present at pH 7.0−7.5 but not under alkaline conditions (pH 8.5−9) (*16*). Our results indicate a significantly higher oligomerization constant [the higher-order species observed by Le Cam et al. (*16*) were obtained at concentrations as low as 180 μM Fur], but this may be related to the use of previously lyophilized protein samples in the mentioned study. The strong influence of the pH on oligomerization can have its origin in protonation, causing neutralization of repulsive charges or leading to additional attractive forces thus enhancing oligomerization. It is likely that the groups involved are histidine side chains. These have a pK_a of around 6.5, and Fur is especially rich in histidine residues (12 histidines per monomer). Moreover, earlier NMR titrations of the Fur histidine residues had shown that seven of the 12 histidines had a pK_a of 6.2−6.7 (*37*). To determine whether oligomerization occurs in vivo, the total concentration of Fur inside the cell has been estimated using the following calculation. The abundance of Fur molecules has been estimated to be ~5000 copies/cell in exponentially growing *E. coli* (*38*) and from 2500 to 7500 copies/cell in *Vibrio cholerae* cultures between their exponential to stationary growing phases (*39*). Under oxidative stress conditions, an amount of 10 000 copies/cell has been reported in *E. coli* (*38*). Considering a maximum variation in cell volume between 3.5×10^{-15} and 1×10^{-15} L in LB medium (*40*), the total Fur concentration inside a single cell is expected in the range of 1−17 μM. This would indicate that higher-order Fur oligomers are most probably not present in vivo. Moreover, considering that K^+, which is the principal monocation present in the cell, is thought to be present at concentrations between 0.1 and 0.5 M (*41*, *42*), the presence of higher-order Fur oligomers is even less likely. However, polymerization of Fur on its cognate DNA in the presence of activating metal has been well established, in vitro, for the aerobactin promoter by electron microscopy and DNAse protection experiments (*15*, *16*). Cooperative binding of additional Fur molecules adjacent to iron box-bound Fur was related to lateral protein−protein interaction (*17*). In addition, it was suggested that this side-by-side oligomerization is correlated to a gradual physiological response to Fe^{2+} (*17*). It is noteworthy that we have identified dimeric, tetrameric, and hexameric species, which may suggest that oligomerization occurs by successive association of dimeric units, possibly related to a side-by-side polymerization on DNA. We have shown here that oligomerization of Fur is significantly more favored at acidic pH. In this respect, it is interesting to note that Fur has been shown to be involved in the acid tolerance response in *E. coli*, *Helicobacter pylori*, and *Salmonella typhimurium* (*10*, *11*, *43*, *44*). In the latter organism, Fur regulates up to 35 genes to maintain a nonlethal intracellular pH (*10*). It is also interesting to note that for its role in acid response, Fur does not require an activating metal (*11*). The pH-regulated oligomerization described here may play a role in the mechanism by which Fur executes its role in acid tolerance response. Size exclusion chromatography shows also the presence of monomeric species during the Fur purification process. This form is not in equilibrium with the dimer, and the properties of the monomer−dimer interconversion have been analyzed.

Reversible Redox- and Zinc-Dependent Dimerization of the Monomer. Purification of Fur from overexpressing cells yields significant amounts of a monomeric form. The purified monomeric species is in an oxidized form containing two disulfide bridges between C92 and C95 and between C132 and C137.

The oxidized monomer (Fur_M^{SS}) can be converted to Fur dimer by DTT-mediated disulfide bridge reduction and subsequent reconstitution with zinc as seen by gel filtration, cross-link experiments, and CD spectroscopy. The CD data clearly show that reduction by DTT did not change the secondary structure of the monomeric Fur, but further addition of Zn^{2+} quantitatively results in formation of the dimer. The dimer formed by reconstitution with zinc exhibits the same metal-dependent DNA binding activity and the same secondary structure as the purified dimer, Zn_1Fur_D. To gain structural information about the binding site in the reduced monomer, Co^{2+} and Fe^{2+} were used as structural probes in place of Zn^{2+}. Fur_M^{SH} was incubated with Co^{2+} and Fe^{2+} instead of Zn^{2+} to generate Co_1Fur_D and Fe_1Fur_D, respectively. These dimeric species display UV−visible and Mössbauer spectroscopic features characteristic of coordination by a sulfur atom in a tetrahedral geometry, indicating that the metal is coordinated in the high-affinity zinc site as seen in the purified dimer Zn_1Fur_D (unpublished data). Therefore, the dimeric species reconstituted by treatment of the oxidized monomer with Zn^{2+} and DTT is entirely consistent with the purified dimer, Zn_1Fur_D. The reduced monomer, Fur_M^{SH}, is unable to dimerize alone but required zinc (or an alternative divalent cation), as demonstrated by gel filtration, cross-link experiments, and CD spectroscopy, indicating that coordination of the zinc ion is the crucial step in dimerization. We also find that although Mn^{2+} can

Scheme 1: Summary of the Various Oligomeric States of Fur and the Factors Involved in Their Interconversion

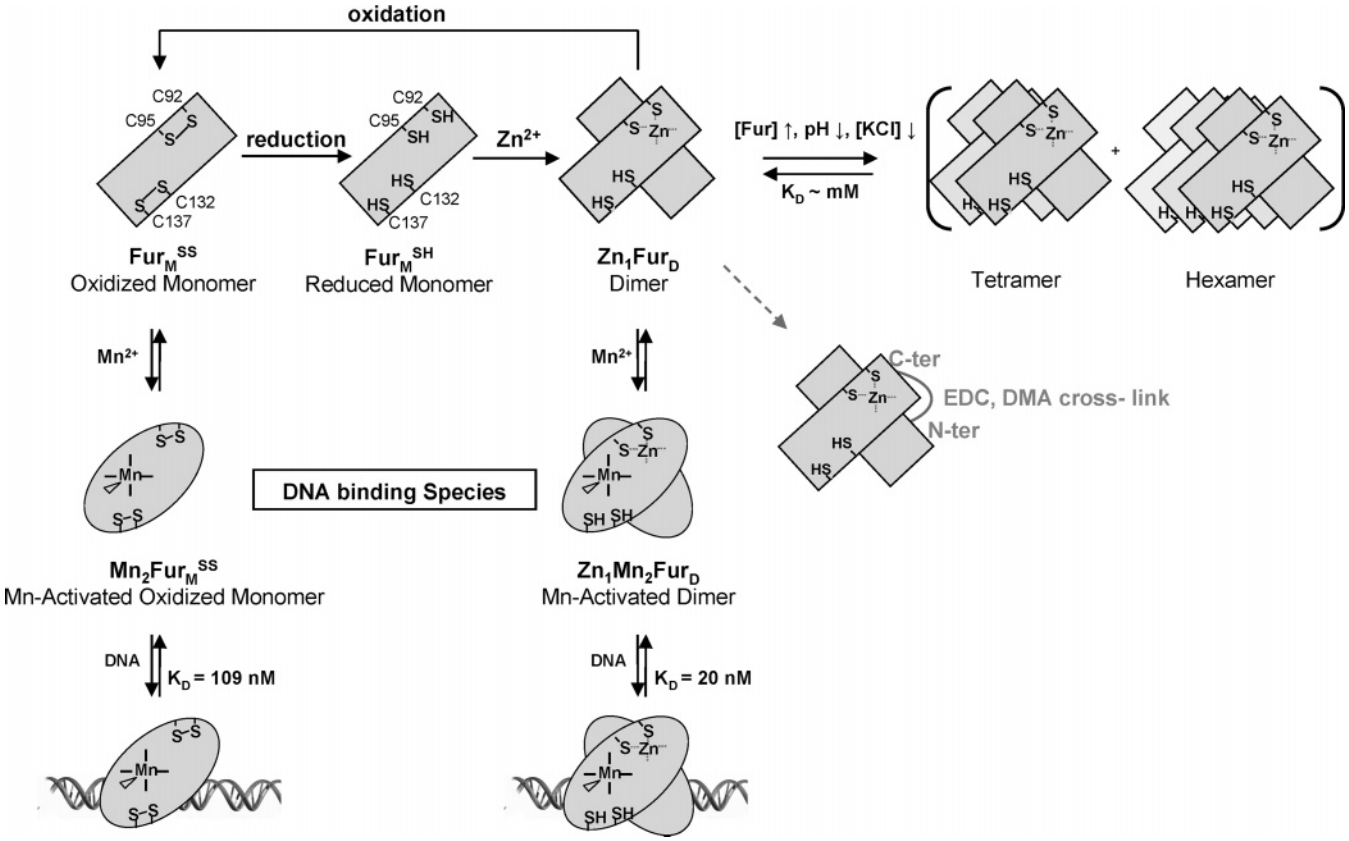

substitute for Zn^{2+} to form a dimer from the reduced monomer, leading to Mn_1Fur_D, it is less efficient. This is probably due to the intrinsic properties of these ions as a tetrahedral site with two thiolates as ligands is more likely to accommodate Zn^{2+} (*45*). Although several divalent cations can trigger dimerization, zinc seems to be favored in vivo as the protein purified in its native form contains zinc ions.

The formation of the oxidized monomer during our purification process may be due to prolonged exposure (>24 h) to a large excess of EDTA [up to 40% of the oxidized monomer at 100 mM EDTA (~5000 equiv of EDTA/Fur)] and/or to oxidation by uncharacterized oxidants in the bacterial extract that may be catalyzed by EDTA. Our conditions are quite different from those described by Althaus et al. (*21*) for a complete removal of zinc from Zn_1Fur_D. These authors did not manage to remove the zinc ion from the structural site in a reaction mixture containing 5000 equiv of EDTA/Fur and 1 mM DTT and incubated overnight. This is probably due to the presence of DTT that is keeping the protein in the reduced form. In contrast, our condition (no DTT with a high concentration of EDTA) allows formation of the oxidized monomer which is devoid of zinc.

It has previously been demonstrated that the Zn^{2+} was bound to C92 and C95 in *E. coli* Fur. Interestingly, the $C^{92}X_2C^{95}$ motif of *E. coli* Fur is highly conserved among microorganisms, suggesting this mechanism of monomer−dimer interconversion may happen with most purified Fur proteins. The Fur protein of *P. aeruginosa* is one of the few examples in which this motif is not conserved with a threonine in place of *E. coli* cysteine 95. A recent biochemical analysis of the Fur protein from *Anabaena* PCC 7119, which contains this motif, suggested that formation of the dimer depends on the oxidation state of the cysteines (*46*). Furthermore, the CX_2C motif is also well-conserved in Fur-like proteins PerR, FurA, CatR, and FurS (*47*−*50*). This indicates that the role of the zinc ion may be well-conserved in the Fur family.

In this paper, we then demonstrate that the high-affinity zinc ion of *E. coli* Fur is essential for upholding the dimeric structure but surprisingly not for DNA binding as we will discuss below.

Role of the Metal Sites in DNA Binding Activity. The fluorescence anisotropy experiments reveal that the oxidized monomer, Fur_M^{SS}, is competent to bind DNA, in a metal-dependent way, as described for the dimer. The Mn^{2+}-activated oxidized monomer ($Mn_2Fur_M^{SS}$) exhibits a 5.5-fold lower apparent affinity for the aerobactin promoter than the Mn^{2+}-activated dimer ($Zn1Mn_2Fur_D$) does. These results indicate first that the zinc site and the reduced thiolates are not required for DNA binding activity. Second, it also demonstrates that the monomer needs a metal activation step as reported for the dimer. We have preliminary data indicating that the affinity of Mn^{2+} for this regulatory site in the oxidized monomer is much lower in comparison to that for the regulatory site in the dimer (unpublished data). Altogether, the DNA binding properties and the metal sensing function of the Fur protein still exist but are altered when it is monomeric. The high values of the Hill coefficients ($n_{dimer} = 1.66 \pm 0.07$ and $n_{monomer} = 2.40 \pm 0.1$) are indicative of a cooperative binding mode, which is more pronounced in the case of the monomer. The cooperativity may be due to the oligomerization of the protein upon DNA binding. In addition, the higher value of the Hill coefficient for the monomer may reflect DNA-assisted dimerization of the

monomer. Therefore, the lower apparent DNA affinity of the monomer may be due to the expense of energy required for dimerization upon DNA binding that is already afforded by Zn^{2+}-dependent stabilization of monomer−monomer contacts in the dimer.

Structural Changes of the Monomer and Dimer upon Metal Binding. To gain insight into the structural changes of the monomer and dimer upon metal activation for their DNA binding, we have performed cross-link experiments and circular dichroism analyses. We have observed that the monomeric forms (Fur_M^{SS} and Fur_M^{SH}) seem less structured than the dimer (CD and ref *51*). Upon dimerization, a significant amount of additional secondary structure is generated that may be related to the long intersubunit β-strand formed at the dimer interface. These results have been confirmed by us in a recent structural study by NMR and X-ray crystallography (*51*) showing that the N-terminal DNA binding domain is well-structured in the monomer and the dimer, contrary to the C-terminal dimerization domain which is structured only in the dimer. In this paper, the analyses of the EDC and DMA cross-linked dimers demonstrate that the N-terminal NH_2 group of one subunit is in an ionic interaction with one or more acidic residues of the C-terminal end and close to Lys76 and Lys97 of the other subunit in the nonactivated dimeric form, Zn_1Fur_D. These cross-links are not observed on the monomer but are quantitatively observed when the oxidized monomer (Fur_M^{SS}) was treated with zinc and reductant to form the dimeric species. Very interestingly, binding of manganese to the dimer Zn_1Fur_D at the regulatory site generating $Zn_1Mn_2Fur_D$ seems to disrupt these interactions since it decreased drastically the cross-link yield. These results are in agreement with the X-ray structure of metal-activated Fur from *P. aeruginosa*, $Zn_1Zn_2Fur_D$, showing that the N-terminal NH_2 group is far from the C-terminal end of the other subunit. Along with the striking observation that the N-terminal end is folded into an α-helix in the oxidized monomeric species and the activated dimer but not in the nonactivated dimer (*51*), the results presented here prompt us to propose that metal binding in the regulatory site destabilizes the intersubunit interaction between C- and N-terminal ends of each monomer (showed by the cross-link data), allowing then the folding of the N-terminal end required for high-affinity DNA binding of the dimer. It is noteworthy that only a dimeric structure will allow an intersubunit contact between C- and N-terminal ends of each monomer and in turn a switch between the folded and unfolded state. The additional α-helix is apparently involved in switching on the DNA binding activity of the Fur protein as it folds upon binding of the metal to the regulatory site. In agreement, it has been reported that the N-terminal helix is required for efficient DNA binding activity and also for specificity (*18*, *52*, *53*). However, although the N-terminal end of the oxidized monomer, Fur_M^{SS}, is folded into an α-helix, as in the activated dimer, we found that the apo oxidized monomer, Fur_M^{SS}, does not bind to DNA but still requires coordination of a metal in its regulatory site to have its DNA binding activity switched on. Therefore, folding of the additional N-terminal helix alone is apparently not enough to promote high-affinity DNA binding to the aerobactin promoter. These results further indicate that metal binding triggers yet unknown changes in the conformation that are required for the DNA binding affinity of the oxidized monomer (*51*). Altogether, these data allowed us to progress in the understanding of the metal-dependent activation mechanisms of the dimer and monomer of Fur in solution.

Role of the Zn Site in Oxidative Stress Sensing. We also present evidence that the dimeric structure of Fur can be directly disrupted following treatment with oxidants such as H_2O_2 or diamide. The in vitro process is accelerated by the presence of EDTA in the case of diamide, indicating that oxidation of the cysteines themselves proceeds faster in the apoprotein. This is further corroborated by the observation that the cysteines involved in binding of the zinc ion, C92 and C95, are air-sensitive ($t_{1/2} = 1$ h) in the reduced monomer, Fur_M^{SH}, whereas they are stable to air when zinc is bound and a dimer is formed, in Zn_1Fur_D. These results indicate that the zinc ion decreases the reactivity of the cysteines toward oxidation by oxygen. The metal-dependent DNA binding activity of the monomer is not precluded but decreased by 5.5-fold in comparison with that of the dimer. As mentioned above, we have preliminary data showing that the affinity of Mn^{2+} for the regulatory site in the oxidized monomer is much lower compared to that for the dimeric form, suggesting that the metal sensing function of Fur is affected by oligomerization state (unpublished data). That distinct feature of the monomeric form is potentially drastic for Fur activity. It is inferred from our results that formation of the monomer may play a role in regulation of Fur activity in response to oxidative stress. However, the existence of the monomeric species, in vivo, is still an unanswered question. It has been reported previously that the cysteines of the purified Fur-like proteins PerR, FurS, and CatR are redox-sensitive and that DTT is able to reverse oxidation, a hallmark of disulfide bridges (*49*, *54*−*56*). In addition, several reports indicate that, in vivo, Fur itself is directly sensitive to oxidants such as H_2O_2 (*57*−*62*). However, a recent in vivo and in vitro study of the Fur-like protein PerR from *Bacillus subtilis* that includes a comparison with *B. subtilis* Fur indicates that the cysteines of Fur and PerR are not oxidized in vivo with mild H_2O_2 treatment (*63*). Instead, peroxide sensing by PerR involves metal-catalyzed oxidation of histidine residue to 2-oxohistidine, but this reaction does not occur with *B. subtilis* Fur. It has been argued that oxidation of cysteine is probably a nonphysiological process occurring only in vitro when a large excess of H_2O_2 is used to oxidize CatR, FurS, and PerR (*63*). Formation of the monomer as we describe here for *E. coli* Fur may explain those results. Our data emphasize that the cysteines of Fur are redox-sensitive. However, assuming a second-order reaction rate constant for the convertion of the dimer in monomer, $k' \sim 0.04$ M^{-1} s^{-1} (estimated from the equation $k = k'[H_2O_2]$, where $k = 0.28 \pm 0.02$ h^{-1}, the pseudo-first-order reaction rate constant, and $[H_2O_2] = 2$ mM), the formation of the monomer appears to be very slow compared to the kinetics of oxidation reported for oxidative stress sensors such as *E. coli* OxyR ($k = 1.1 \times 10^5$ M^{-1} s^{-1}) (*64*) and *B. subtilis* PerR ($k \sim 10^5$ M^{-1} s^{-1}) (*63*). The rate of monomer formation is much more closer to those reported for other $Zn(Cys)_n$-containing oxidative stress sensors such as Hsp33, a redox-regulated molecular chaperone, and RsrA, a redox-regulated anti-σ factor (*65*, *66*). The bimolecular reaction rate of the reaction of H_2O_2 with *E. coli* Hsp33 and diamide with *Streptomyces coelicolor* RsrA could be esti-

mated using the previously reported $t_{1/2}$ for expulsion of zinc upon oxidation (*65*, *66*). The reaction rate predicted from calculation for oxidation of Hsp33 by H_2O_2 at 43 °C is $k = 0.36\ M^{-1}\ s^{-1}$ and for oxidation of RsrA by diamide is $0.11\ M^{-1}\ s^{-1}$. These reaction rates are 10^5-10^6-fold below those reported for OxyR and PerR but only 3−10-fold higher than the one reported here for Fur, indicating that Fur may share similar properties with these stress sensors. However, the low reaction rate with H_2O_2 indicates that the zinc site of Fur is a poor sensor of hydrogen peroxide and that sensing of hydrogen peroxide by the Fur-like protein through thiol−disulfide switch, zinc expulsion, and dimer−monomer transition may be only a mechanism of regulation under severe and/or prolonged exposure to hydrogen peroxide as proposed for the structural zinc site of *B. subtilis* PerR under iron-starved conditions (*67*). Alternately, the zinc site of Fur may sense ill-defined redox active signals that could react faster with the zinc site to trigger the dimer−monomer transition. Finally, our results suggest that the structural zinc ion has probably evolved as a robust quaternary structure element that is crucial for upholding the dimeric structure of Fur and ensuring efficient iron sensing and specificity of the Fur repressor.

ACKNOWLEDGMENT

We are indebted to Julien Viret and Colette Lebrun for their help in the experimental work.

SUPPORTING INFORMATION AVAILABLE

Description of the calculation applied to the oligomeric equilibrium and two tables and one figure related to the mass analyses of the cross-linked experiments. This material is available free of charge via the Internet at http://pubs.acs.org.

REFERENCES

1. Hantke, K. (2001) Iron and metal regulation in bacteria, *Curr. Opin. Microbiol. 4*, 172−177.
2. Angerer, A., and Braun, V. (1998) Iron regulates transcription of the *Escherichia coli* ferric citrate transport genes directly and through the transcription initiation proteins, *Arch. Microbiol. 169*, 483−490.
3. Escolar, L., Perez-Martin, J., and de Lorenzo, V. (1999) Opening the iron box: Transcriptional metalloregulation by the Fur protein, *J. Bacteriol. 181*, 6223−6229.
4. Touati, D. (2000) Iron and oxidative stress in bacteria, *Arch. Biochem. Biophys. 373*, 1−6.
5. de Lorenzo, V., Wee, S., Herrero, M., and Neilands, J. B. (1987) Operator sequences of the aerobactin operon of plasmid ColV-K30 binding the ferric uptake regulation (Fur) repressor, *J. Bacteriol. 169*, 2624−2630.
6. Calderwood, S. B., and Mekalanos, J. L. (1988) Confirmation of the Fur operator site by insertion of a synthetic oligonucleotide into an operon fusion plasmid, *J. Bacteriol. 170*, 1015−1017.
7. D'Autréaux, B., Touati, D., Bersch, B., Latour, J. M., and Michaud-Soret, I. (2002) Direct inhibition by nitric oxide of the transcriptional ferric uptake regulation protein via nitrosylation of the iron, *Proc. Natl. Acad. Sci. U.S.A. 99*, 16619−16624.
8. D'Autréaux, B., Horner, O., Oddou, J. L., Jeandey, C., Gambarelli, S., Berthomieu, C., Latour, J. M., and Michaud-Soret, I. (2004) Spectroscopic description of the two nitrosyl-iron complexes responsible for Fur inhibition by nitric oxide, *J. Am. Chem. Soc. 126*, 6005−6016.
9. Mukhopadhyay, P., Zheng, M., Bedzyk, L. A., LaRossa, R. A., and Storz, G. (2004) Prominent roles of the NorR and Fur regulators in the *Escherichia coli* transcriptional response to reactive nitrogen species, *Proc. Natl. Acad. Sci. U.S.A. 101*, 745−750.
10. Foster, J. W., and Hall, H. K. (1992) Effect of *Salmonella typhimurium* ferric uptake regulator (fur) mutations on iron- and pH-regulated protein synthesis, *J. Bacteriol. 174*, 4317−4323.
11. Hall, H. K., and Foster, J. W. (1996) The role of Fur in the acid tolerance response of *Salmonella typhimurium* is physiologically and genetically separable from its role in iron acquisition, *J. Bacteriol. 178*, 5683−5691.
12. Neilands, J. B., and Nakamura, K. (1991) Detection, determination, isolation, characterization and regulation of microbial iron chelates, in *CRC Handbook of Microbial Iron Chelates* (Winkelmann, G., Ed.) pp 1−14, CRC Press, Boca Raton, FL.
13. Michaud-Soret, I., Adrait, A., Jaquinod, M., Forest, E., Touati, D., and Latour, J. M. (1997) Electrospray ionization mass spectrometry analysis of the apo- and metal-substituted forms of the Fur protein, *FEBS Lett. 413*, 473−476.
14. Braun, V., Schäffer, S., Hantke, K., and Tröger, W. (1990) Regulation of gene expression by iron, in *The molecular basis of bacterial metabolism. Colloquium Mosbach 1990*, pp 165−179, Springer-Verlag, Berlin.
15. Frechon, D., and Le Cam, E. (1994) FUR (ferric uptake regulation) protein interaction with target DNA: Comparison of gel retardation, footprinting and electron microscopy analyses, *Biochem. Biophys. Res. Commun. 201*, 346−355.
16. Le Cam, E., Frechon, D., Barray, M., Fourcade, A., and Delain, E. (1994) Observation of binding and polymerization of Fur repressor onto operator-containing DNA with electron and atomic force microscopes, *Proc. Natl. Acad. Sci. U.S.A. 91*, 11816−11820.
17. Escolar, L., Perez-Martin, J., and de Lorenzo, V. (2000) Evidence of an unusually long operator for the Fur repressor in the aerobactin promoter of *Escherichia coli*, *J. Biol. Chem. 275*, 24709−24714.
18. Pohl, E., Haller, J. C., Mijovilovich, A., Meyer-Klaucke, W., Garman, E., and Vasil, M. L. (2003) Architecture of a protein central to iron homeostasis: Crystal structure and spectroscopic analysis of the Ferric uptake regulator, *Mol. Microbiol. 47*, 903−915.
19. Jacquamet, L., Aberdam, D., Adrait, A., Hazemann, J. L., LAtour, J. M., and Michaud-Soret, I. (1998) X-ray absorption spectroscopy of a new zinc site in the Fur protein from *Escherichia coli*, *Biochemistry 37*, 2564−2571.
20. Adrait, A., Jacquamet, L., Le Pape, L., Gonzalez de Peredo, A., Aberdam, D., Hazemann, J. L., Latour, J. M., and Michaud-Soret, I. (1999) Spectroscopic and saturation magnetization properties of the manganese and cobalt substituted Fur (ferric uptake regulation) protein from *Escherichia coli*, *Biochemistry 38*, 6248−6260.
21. Althaus, E. W., Outten, C. E., Olson, K. E., Cao, H., and O'Halloran, T. V. (1999) The ferric uptake regulation (Fur) repressor is a zinc metalloprotein, *Biochemistry 38*, 6559−6569.
22. Jacquamet, L., Dole, F., Jeandey, C., Oddou, J. L., Perret, E., Le Pape, L., Aberdam, D., Hazemann, J. L., Michaud-Soret, I., and Latour, J. M. (2000) First spectroscopic characterization of Fe(II)-Fur, the physiological active form of the Fur protein, *J. Am. Chem. Soc. 122*, 394−395.
23. Gonzalez de Peredo, A., Saint-Pierre, C., Adrait, A., Jacquamet, L., Latour, J. M., Forest, E., and Michaud-Soret, I. (1999) Identification of the two zinc-bound cysteines in the ferric uptake regulation protein from *Escherichia coli*: Chemical modification and mass spectrometry analysis, *Biochemistry 38*, 8582−8589.
24. Coy, M., Doyle, C., Besser, J., and Neilands, J. B. (1994) Site-directed mutagenesis of the ferric uptake regulation gene of *Escherichia coli*, *BioMetals 7*, 292−298.
25. Lewin, A. C., Doughty, P. A., Flegg, L., Moore, G. R., and Spiro, S. (2002) The ferric uptake regulator of *Pseudomonas aeruginosa* has no essential cysteine residues and does not contain a structural zinc ion, *Microbiology 148*, 2449−2456.
26. Wee, S., Neilands, J. B., Bittner, M. L., Hemming, B. C., Haymore, B. L., and Seetharam, R. (1988) Expression, isolation and properties of Fur (ferric uptake regulation) protein of *Escherichia coli* K 12, *Biol. Met. 1*, 62−68.
27. Manning, L. R., Jenkins, W. T., Hess, J. R., Vandegriff, K., Winslow, R. M., and Manning, J. M. (1996) Subunit dissociations in natural and recombinant hemoglobins, *Protein Sci. 5*, 775−781.
28. Andreeva, A. L., Andreev, O. A., and Borejdo, J. (1993) Structure of the 265-kilodalton complex formed upon EDC cross-linking of subfragment 1 to F-actin, *Biochemistry 32*, 13956−13960.

29. Dallmann, H. G., Flynn, T. G., and Dunn, S. D. (1992) Determination of the 1-ethyl-3-[(3-dimethylamino)propyl]-carbodiimide-induced cross-link between the β and ϵ subunits of *Escherichia coli* F1-ATPase, *J. Biol. Chem. 267*, 18953−18960.
30. Lacroix, M., Rossi, V., Gaboriaud, C., Chevallier, S., Jaquinod, M., Thielens, N. M., Gagnon, J., and Arlaud, G. J. (1997) Structure and assembly of the catalytic region of human complement protease C1r: A three-dimensional model based on chemical cross-linking and homology modeling, *Biochemistry 36*, 6270−6282.
31. Tiss, A., Barre, O., Michaud-Soret, I., and Forest, E. (2005) Characterization of the DNA-binding site in the ferric uptake regulator protein from *Escherichia coli* by UV crosslinking and mass spectrometry, *FEBS Lett. 579*, 5454−5460.
32. Mills, S. A., and Marletta, M. A. (2005) Metal binding characteristics and role of iron oxidation in the ferric uptake regulator from *Escherichia coli*, *Biochemistry 44*, 13553−13559.
33. Smith, A., Hooper, N. I., Shipulina, N., and Morgan, W. T. (1996) Heme binding by a bacterial repressor protein, the gene product of the ferric uptake regulation (fur) gene of *Escherichia coli*, *J. Protein Chem. 15*, 575−583.
34. Hamed, M. Y., and Neilands, J. B. (1994) An electron spin resonance study of the Mn(II) and Cu(II) complexes of the Fur repressor protein, *J. Inorg. Biochem. 53*, 235−248.
35. Li, R., Nagai, Y., and Nagai, M. (2000) Changes of tyrosine and tryptophan residues in human hemoglobin by oxygen binding: Near- and far-UV circular dichroism of isolated chains and recombined hemoglobin, *J. Inorg. Biochem. 82*, 93−101.
36. Sreerama, N., and Woody, R. W. (2004) Computation and analysis of protein circular dichroism spectra, *Methods Enzymol. 383*, 318−351.
37. Saito, T., Duly, D., and Williams, R. P. J. (1991) The histidines of the iron-uptake regulation protein, Fur, *Eur. J. Biochem. 197*, 39−42.
38. Zheng, M., Doan, B., Schneider, T. D., and Storz, G. (1999) OxyR and SoxRS regulation of fur, *J. Bacteriol. 181*, 4639−4643.
39. Watnick, P. I., Eto, T., Takahashi, H., and Calderwood, S. B. (1997) Purification of *Vibrio cholerae* Fur and estimation of its intracellular abundance by antibody sandwich enzyme-linked immunosorbent assay, *J. Bacteriol. 179*, 243−247.
40. Ali Azam, T., Iwata, A., Nishimura, A., Ueda, S., and Ishihama, A. (1999) Growth phase-dependent variation in protein composition of the *Escherichia coli* nucleoid, *J. Bacteriol. 181*, 6361−6370.
41. Bremer, H., Dennis, P. P., and Neidhardt, F. C. (1996) *Escherichia coli and Salmonella: Cellular and Molecular Biology*, Vol. 2, ASM Press, Washington, DC.
42. Outten, C. E., and O'Halloran, T. V. (2001) Femtomolar sensitivity of metalloregulatory proteins controlling zinc homeostasis, *Science 292*, 2488−2492.
43. Audia, J. P., Webb, C. C., and Foster, J. W. (2001) Breaking through the acid barrier: An orchestrated response to proton stress by enteric bacteria, *Int. J. Med. Microbiol. 291*, 97−106.
44. Bijlsma, J. J., Waidner, B., Vliet, A. H., Hughes, N. J., Hag, S., Bereswill, S., Kelly, D. J., Vandenbroucke-Grauls, C. M., Kist, M., and Kusters, J. G. (2002) The *Helicobacter pylori* homologue of the ferric uptake regulator is involved in acid resistance, *Infect. Immun. 70*, 606−611.
45. Berg, J. M., and Shi, Y. (1996) The galvanization of biology: A growing appreciation for the roles of zinc, *Science 271*, 1081−1085.
46. Hernandez, J. A., Bes, M. T., Fillat, M. F., Neira, J. L., and Peleato, M. L. (2002) Biochemical analysis of the recombinant Fur (ferric uptake regulator) protein from *Anabaena* PCC 7119: Factors affecting its oligomerization state, *Biochem. J. 366*, 315−322.
47. van Vliet, A. H., Baillon, M. L., Penn, C. W., and Ketley, J. M. (1999) *Campylobacter jejuni* contains two Fur homologs: Characterization of iron-responsive regulation of peroxide stress defense genes by the PerR repressor, *J. Bacteriol. 181*, 6371−6376.
48. Pagan-Ramos, E., Song, J., McFalone, M., Mudd, M. H., and Deretic, V. (1998) Oxidative stress response and characterization of the oxyR-ahpC and furA-katG loci in *Mycobacterium marinum*, *J. Bacteriol. 180*, 4856−4864.
49. Hahn, J. S., Oh, S. Y., Chater, K. F., Cho, Y. H., and Roe, J. H. (2000) H_2O_2-sensitive Fur-like repressor CatR regulating the major catalase gene in *Streptomyces coelicolor*, *J. Biol. Chem. 275*, 38254−38260.
50. Zou, P., Borovok, I., Ortiz de Orue Lucana, D., Muller, D., and Schrempf, H. (1999) The mycelium-associated *Streptomyces reticuli* catalase-peroxidase, its gene and regulation by FurS, *Microbiology 145* (Part 3), 549−559.
51. Pecqueur, L., D'Autréaux, B., Dupuy, J., Nicolet, Y., Jacquamet, L., Brutscher, B., Michaud-Soret, I., and Bersch, B. (2006) Structural changes of *Escherichia coli* ferric uptake regulator during metal-dependent dimerization and activation explored by NMR and X-ray crystallography, *J. Biol. Chem. 281*, 21286−21295.
52. Coy, M., and Neilands, J. B. (1991) Structural dynamics and functional domains of the Fur protein, *Biochemistry 30*, 8201−8210.
53. Barton, H. A., Johnson, Z., Cox, C. D., Vasil, A. I., and Vasil, M. L. (1996) Ferric uptake regulator mutants of *Pseudomonas aeruginosa* with distinct alterations in the iron-dependent repression of exotoxin A and siderophores in aerobic and microaerobic environments, *Mol. Microbiol. 21*, 1001−1017.
54. Ortiz de Orue Lucana, D., and Schrempf, H. (2000) The DNA-binding characteristics of the *Streptomyces reticuli* regulator FurS depend on the redox state of its cysteine residues, *Mol. Gen. Genet. 264*, 341−353.
55. Ortiz de Orue Lucana, D., Troller, M., and Schrempf, H. (2003) Amino acid residues involved in reversible thiol formation and zinc ion binding in the *Streptomyces reticuli* redox regulator FurS, *Mol. Genet. Genomics 268*, 618−627.
56. Herbig, A. F., and Helmann, J. D. (2001) Roles of metal ions and hydrogen peroxide in modulating the interaction of the *Bacillus subtilis* PerR peroxide regulon repressor with operator DNA, *Mol. Microbiol. 41*, 849−859.
57. Lee, J. H., Yeo, W. S., and Roe, J. H. (2004) Induction of the sufA operon encoding Fe-S assembly proteins by superoxide generators and hydrogen peroxide: Involvement of OxyR, IHF and an unidentified oxidant-responsive factor, *Mol. Microbiol. 51*, 1745−1755.
58. Mostertz, J., Scharf, C., Hecker, M., and Homuth, G. (2004) Transcriptome and proteome analysis of *Bacillus subtilis* gene expression in response to superoxide and peroxide stress, *Microbiology 150*, 497−512.
59. Zeller, T., Moskvin, O. V., Li, K., Klug, G., and Gomelsky, M. (2005) Transcriptome and physiological responses to hydrogen peroxide of the facultatively phototrophic bacterium *Rhodobacter sphaeroides*, *J. Bacteriol. 187*, 7232−7242.
60. Zheng, M., Wang, X., Doan, B., Lewis, K. A., Schneider, T. D., and Storz, G. (2001) Computation-directed identification of OxyR DNA binding sites in *Escherichia coli*, *J. Bacteriol. 183*, 4571−4579.
61. Grifantini, R., Frigimelica, E., Delany, I., Bartolini, E., Giovinazzi, S., Balloni, S., Agarwal, S., Galli, G., Genco, C., and Grandi, G. (2004) Characterization of a novel *Neisseria meningitidis* Fur and iron-regulated operon required for protection from oxidative stress: Utility of DNA microarray in the assignment of the biological role of hypothetical genes, *Mol. Microbiol. 54*, 962−979.
62. Pomposiello, P. J., Bennik, M. H., and Demple, B. (2001) Genome-wide transcriptional profiling of the *Escherichia coli* responses to superoxide stress and sodium salicylate, *J. Bacteriol. 183*, 3890−3902.
63. Lee, J. W., and Helmann, J. D. (2006) The PerR transcription factor senses H_2O_2 by metal-catalysed histidine oxidation, *Nature 440*, 363−367.
64. Lee, C., Lee, S. M., Mukhopadhyay, P., Kim, S. J., Lee, S. C., Ahn, W. S., Yu, M. H., Storz, G., and Ryu, S. E. (2004) Redox regulation of OxyR requires specific disulfide bond formation involving a rapid kinetic reaction path, *Nat. Struct. Mol. Biol. 11*, 1179−1185.
65. Jakob, U., Eser, M., and Bardwell, J. C. (2000) Redox switch of hsp33 has a novel zinc-binding motif, *J. Biol. Chem. 275*, 38302−38310.
66. Li, W., Bottrill, A. R., Bibb, M. J., Buttner, M. J., Paget, M. S., and Kleanthous, C. (2003) The role of zinc in the disulphide stress-regulated anti-σ factor RsrA from *Streptomyces coelicolor*, *J. Mol. Biol. 333*, 461−472.
67. Lee, J. W., and Helmann, J. D. (2006) Biochemical characterization of the structural Zn^{2+} site in the *Bacillus subtilis* peroxide sensor PerR, *J. Biol. Chem. 281*, 23567−23578.

BI061636R